Rare Metal Materials and Engineering
Volume 54, Issue 1, January 2025
Available online at www.rmme.ac.cn

Science Press

Cite this article as: Wang Xingxing, Chu Haoqiang, Xie Xu, et al. Advancement in Tungsten/Molybdenum Alloy Welding Technology[J]. Rare Metal Materials and Engineering, 2025, 54(01): 94-108. DOI: 10.12442/j.issn.1002-185X.20240462.

REVIEW

Advancement in Tungsten/Molybdenum Alloy Welding Technology

Wang Xingxing[1], Chu Haoqiang[1], Xie Xu[1], Pan Kunming[2], Du Quanbin[3], Li Ang[3], Zhang Liyan[3]

[1] Henan International Joint Laboratory of High-efficiency Special Green Welding, North China University of Water Resources and Electric Power, Zhengzhou 450045, China; [2] Longmen Laboratory, Luoyang 471003, China; [3] Henan Key Laboratory of Intelligent Manufacturing Equipment Integration for Superhard Materials, Henan Mechanical and Electrical Vocational College, Zhengzhou 451191, China

Abstract: Tungsten/molybdenum alloys are widely utilized in the nuclear industry, aerospace and various other fields due to their high melting points and strength characteristics. However, poor sinterability and processability make it difficult to manufacture large-size or complex-shaped parts. Hence, an in-depth study on the welding technology of tungsten/molybdenum alloys is urgent. An introduction of tungsten/molybdenum alloy welding defects and joining process was provided, along with recent advancements in brazing, spark plasma sintering diffusion bonding, electron beam welding and laser beam welding. The latest progress in alloy doping treatment applied to tungsten/molybdenum alloy dissimilar welding was also discussed, and existing welding problems were pointed out. The development prospects of weldability of tungsten/molybdenum alloy by various joining technologies were forecasted, thereby furnishing a theoretical and practical found.

Key words: tungsten alloy; molybdenum alloy; welding technology; microstructure; mechanical properties

Molybdenum alloys possess unique properties, such as high melting point, high strength, high corrosion resistance, good thermal and electrical conductivity, which have been widely used in nuclear energy, shipbuilding, aerospace and petrochemicals (e. g., rocket nozzle throats and nuclear fuel rod sets) [1–2]. Tungsten alloys are characterized by high modulus of elasticity, low coefficient of thermal expansion, excellent high-temperature strength and thermal stability, which can be applied in chemical industry, mining, metallurgy, etc[3–5]. In harsh working environment, tungsten alloys and molybdenum alloys have unique advantages so they are difficult to replace. There are vigorous related research on improvement of the applicability and breadth of their field applications[6]. Refractory metal components are usually manufactured by powder metallurgy. However, such technology is unable to meet the manufacturing requirements for large and complex-shaped tungsten/molybdenum alloy structural components. Consequently, new welding techniques need to be developed to produce necessary components[7–8].

Tungsten alloy and molybdenum alloy are characterized by high brittleness, low ductile-brittle transition temperature and poor weld ability[9]. Simultaneously, tungsten alloy and molybdenum alloy matrices are usually produced by powder metallurgy techniques, which are more prone to impurities and gases compared with melting metallurgy. Notably, oxygen reacts with molybdenum to form molybdenum oxide, causing crack and brittle fracture for tungsten/molybdenum welded joints, which in turn increases the failure risk in critical applications[10]. To avoid such scenario, advanced welding techniques, such as brazing, spark plasma sintering (SPS) diffusion welding, electron beam welding (EBW), and laser beam welding (LBW) are widely employed for joining tungsten/molybdenum alloys, in order to achieve high-quality joints with excellent microstructure and mechanical properties.

Received date: July 27, 2024
Foundation item: National Natural Science Foundation of China (52071165, 52475347); National Program of Foreign Experts of China (G2023026003L); China Postdoctoral Fund (2023M740475); Program for Science & Technology Innovation Talents in Universities of Henan Province, China (22HASTIT026); Program for the Top Young Talents of Henan Province, China; Frontier Exploration Projects of Longmen Laboratory, China (LMQYTSKT016); Key Scientific Research Projects of Colleges and Universities in Henan Province, China (24A460008); Key Science and Technology Project of Henan Province, China (242102220064, 222102230111)
Corresponding author: Wang Xingxing, Ph. D., Professor, Henan International Joint Laboratory of High-efficiency Special Green Welding, North China University of Water Resources and Electric Power, Zhengzhou 450045, P. R. China, E-mail: wangxingxing@ncwu.edu.cn

Brazing is a method in which low-melting-point filler metal is melted and used to fill the gaps between solid workpieces. Part of defects during weld processes can be avoided by choosing appropriate brazing material. Additionally, the formation of brittle phase can be suppressed by adjusting the brazing material and soldering temperature[11]. However, brazing takes too long time to meet the demand of mass production and tungsten/molybdenum alloys exhibit low coefficients of thermal expansion. The joints after welding may have stress concentrations due to uneven thermal expansion, which results in brittle welds. EBW and LBW produce a large amount of heat energy through the focusing of the electron beam or light beam to melt the surface of the workpiece and to form a weld. Due to the advantages of fast welding speed, small heat-affected zone (HAZ) and small welding stress and deformation, they can be used for thicker tungsten/molybdenum alloys and have a significant advantage for welding brittle alloys of the tungsten/molybdenum class with high thermal conductivity[12–13]. The adjustment of welding parameters and intermediate layer metals can effectively refine grain size and reduce porosity defects and intermetallic compounds[14–15]. However, the fusion welding joints, including EBW and LBW, are rougher and easier to form coarse grain size due to high heat input, which increases brittleness of the joint. SPS diffusion welding is an advanced method with extremely rapid development. Fine-crystalline tungsten alloys and molybdenum alloys can achieve rapid densification at lower sintering temperatures and shorten sintering time, obtaining ultra-high-quality joints[16–17]. However, it cannot satisfy the welding needs of large, complex-shaped structural parts. The common challenges in tungsten/molybdenum alloy welding is follows: the suppression of brittle compounds and oxides, the refinement of grain structure, and the reduction of residual stresses. Additionally, achieving a more flexible, efficient and user-friendly welding process is also contained.

This study started from the welding defects of tungsten alloy and molybdenum alloy, summarized the research status of brazing, SPS diffusion welding, EBW, and LBW in the field of tungsten alloy and molybdenum alloy welding, and looked forward to the development trend. The definitive purpose is to provide a theoretical basis and technical support for the research and application of tungsten/molybdenum alloy welded joints in related fields.

1 Tungsten/Molybdenum Alloy Welded Joint Defects

Tungsten/molybdenum alloy joints suffer from two major defects: brittleness and porosity. There are two main reasons for brittleness. Firstly, tungsten and molybdenum alloys are inherently brittle; secondly, the heat input of different welding methods affects the grain size, leading to varying degrees of brittleness in the joint. Micropores generated during powder metallurgy preparation absorbed impurities and inadequate weld preparation can introduce gas into the molten pool. Incomplete gas drainage from the joint during solidification leads to porosity.

1.1 Brittleness

1.1.1 Room temperature brittleness

Due to high ductile-to-brittle transition temperature of tungsten alloys and molybdenum alloys, they exhibit brittleness at room temperature. The primary intrinsic reason is the half-filled electron distribution characteristics of the outermost and penultimate atomic layers[18]. The ductile-brittle transition temperature of tungsten is generally around 600 °C, and that of molybdenum is in the range of 140 °C to 150 °C, which restricts their applications in low-temperature environment.

1.1.2 Effect of impurities on brittleness

Manufactured by powder metallurgy, tungsten alloy and molybdenum alloy contain interstitial impurities (C, N, O, P, etc). During the welding process, some impurities entering the molten pool are diffused and enriched sufficiently along the grain boundaries, which will weaken the interfacial bonding. Oxygen has the most significant effect in this regard. At a microscopic level, the enrichment of trace interstitial impurities along the grain boundaries prompts the generation of the second phase (MoO_2 and WO_2). As depicted in Fig.1[19], during LBW processes, microstructures at the fracture contain a large number of MoO_2, significantly weakening the grain boundary bonding force, which is detrimental to the overall performance of the welded joints[20]. Impurity segregation at the grain boundaries of the material increases the susceptibility to weld cracking and severely reduces the performance of tungsten and molybdenum alloy joints in terms of strength, malleability and ductility[21–22].

1.1.3 Effect of welding method on brittleness

Weld embrittlement is mainly caused by the difference in strength between the weld metal and base metal (BM). The

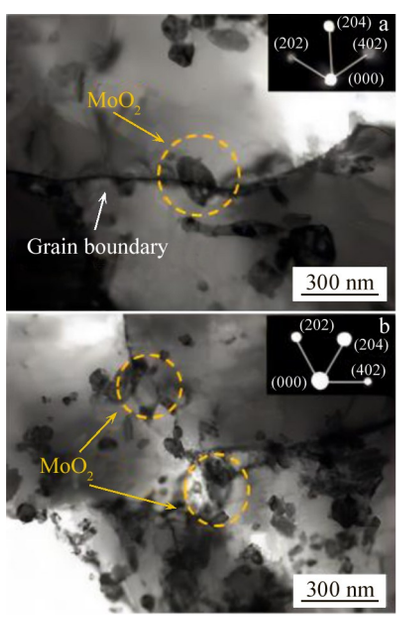

Fig.1 TEM images of fusion zone of laser welded Mo alloy joints with different heat inputs: (a) 250 J/cm and (b) 3600 J/cm[19]

variance in heat input among different welding methods significantly affects the microstructure of BM and HAZ, thereby resulting in different mechanical properties. The main causes of brittleness at the interface are coarse grain and the formation of brittle intermetallics and oxides. Brazing has relatively low heat input, and the joints experience less thermal stress during the welding process, resulting in relatively fewer problems of coarse grain. However, localized embrittlement still occurs if compatibility between the brazing material and BM is poor or if a large number of impurities are presented[23–24]. Tungsten and molybdenum, as refractory metals, are difficult to melt and to bond effectively with other metals. Therefore, Ni-based, Ti-based and other active solders are commonly used. However, brittle Ni-Ti compounds obviously form at the welded interface after welding. SPS diffusion welding is characterized by fast heating speed, relatively concentrated heat input, and more uniform overall heating process, which reduces the temperature gradient in the welding area, thereby effectively reducing the brittleness of welded joint. As depicted in Fig.2[25], due to high energy input and localized heating, EBW and LBW are prone to rapid cooling and large temperature gradients in the weld zone (WZ), which can lead to excessive grain growth and abnormal grain boundary structure, thereby increasing the formation of brittleness microstructures. Laser welding in a non-vacuum environment often leads to the formation of MoO_2, which adversely affects the mechanical properties of the joint. To inhibit MoO_2, Ti, Zr and other elements are added to the intermediate layer. Since TiO_2 and ZrO_2 have lower Gibbs free energy, they can form preferentially and provide stronger bonding at the grain boundaries.

1.2 Stomata

Tungsten/molybdenum alloys usually suffer from porosity defects during welding processes, which seriously deteriorates the weld quality of the joints. As shown in Fig.2a, weld pores are gathered at the grain boundaries in the WZ. Moisture and gases in the BM, doped oxides, shielding gas and impurities (e.g., rust, oil) in the joint can generate gas and enter into the molten pool[26]. At high temperatures, the solubility of gas is high, and as the solidification process progresses, the viscosity of the liquid metal gradually increases, reducing the escaping rate of gas. When the liquid metal is cooled, the gas is still difficult to expel, resulting in the formation of pores at the grain boundaries in the WZ, which severely deteriorates the quality of weld joints[27].

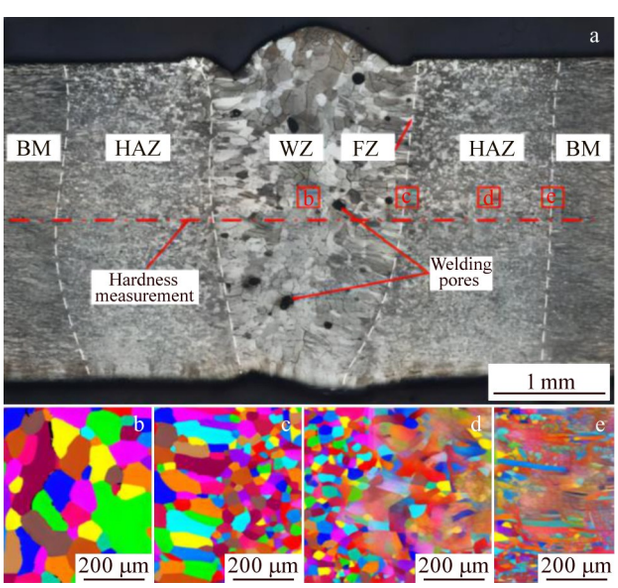

Fig.2 Microstructures of EBWed TZM alloy joints: (a) weld cross section, (b) WZ, (c) FZ, (d) HAZ, and (e) BM (regions b–e in Fig.2a correspond to Fig.2b–2e, respectively)[25]

2 Advancement in Welding Research of Tungsten and Molybdenum Alloys

At present, tungsten/molybdenum alloy welding methods mainly include brazing, SPS diffusion welding, EBW, and LBW. The advantages and disadvantages of different welding methods, as well as their improvements and developments, are shown in Fig.3[28–32]. An overview of the mechanical properties is presented in Table 1[33–58].

2.1 Brazing

Brazing is one of the most commonly used methods for joining tungsten/molybdenum alloy dissimilar materials as it has the advantages of low operating temperature, small thermal effects, flat and smooth joints, and small residual stress deformation in the BM[28–29]. The difficulty of brazing tungsten/molybdenum alloy dissimilar joints lay in controlling the intergranular infiltration behavior and suppressing the precipitation of brittle phases, for which it is necessary to select suitable brazing materials and process, including weld temperature and hold time. The brazing materials used in tungsten/molybdenum alloy are mainly Ag-based, Au-based, Ti-based and Ni-based materials. Compared with Ag-based and Au-based materials, Ti-based and Ni-based materials are widely used because of good high temperature performances and economy[30–32].

Lu et al[33] investigated the effect of Ni-44Ti and Ni-13.7Ti brazing materials on the intergranular infiltration of TZM brazed joints. The results show that different ratios of Ti and Ni affect the intergranular penetration behavior, resulting in brazed joints with varying strengths. The shear strength of TZM/Ni-13.7Ti/TZM brazed joints is 193 MPa, while the shear strength of TZM/Ni-44Ti/TZM brazed joints is 167 MPa. Han et al[34–35] used Ti-28Ni eutectic material to braze TZM alloy and ZrC_p-W. It is shown that different brazing temperatures induce an increasing and then decreasing tendency for the joint strength. The room temperature shear strength of the specimen reached 120.5 MPa after brazing at 1040 °C for 10 min, and the highest shear strength of the specimen reached 77.5 MPa at 800 °C in high-temperature environment. Han et al[36] used Ti-61Ni to braze TZM alloys and ZrC_p-W composites under vacuum at 1240 °C, and the optimum shear strengths reached 124.8 MPa at room temperature and 82.3 MPa at 800 °C, representing an incre-

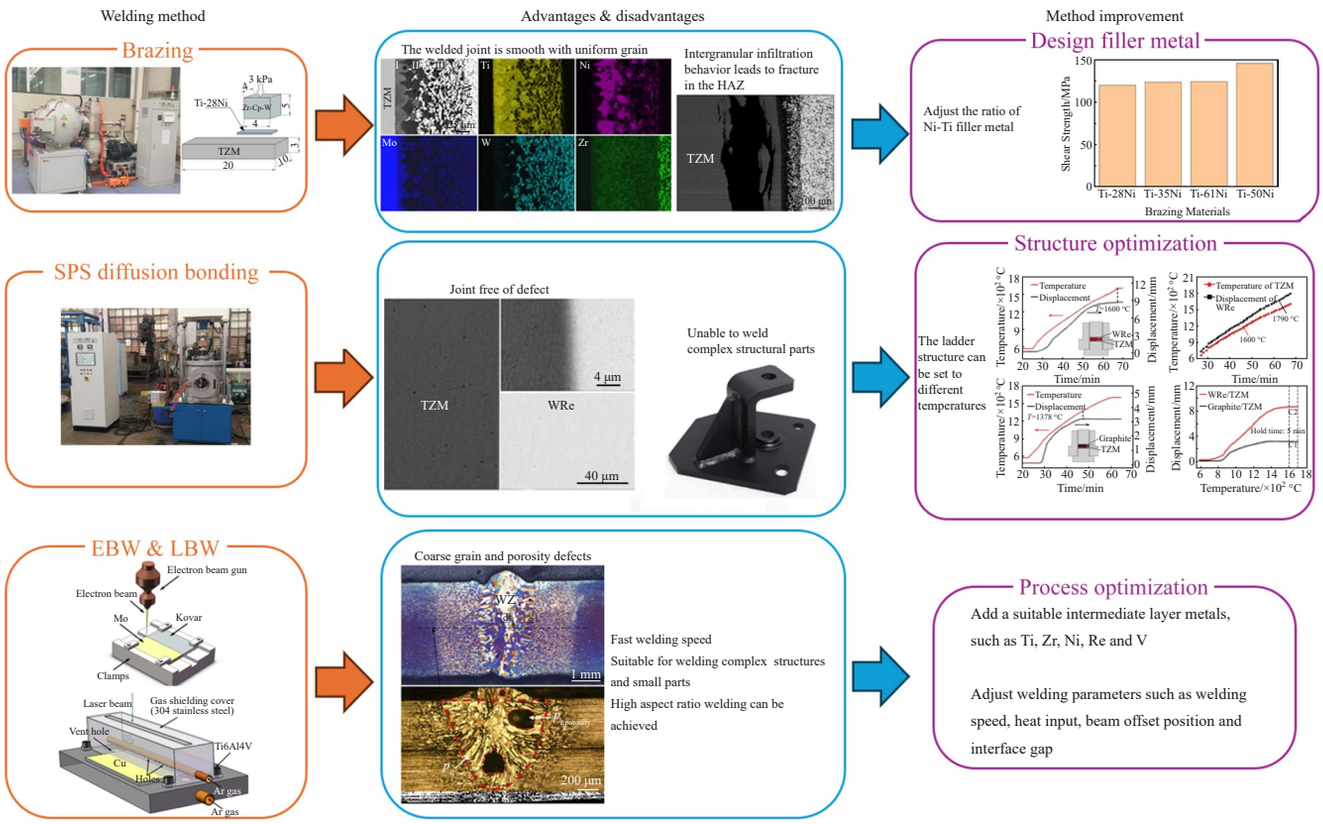

Fig.3 Characteristics of different welding methods for tungsten/molybdenum alloys[28–32]

ment of 3.6% and 6.1% in shear strength compared to those of Ti-28Ni brazing material, respectively. Song et al[37] employed Ti-35Ni material to braze TZM alloy with ZrC_p-W composite. The maximum average shear strengths were 123.8 MPa at room temperature and 110.2 MPa at 800 °C. When the braze condition was 1260 °C for 10 min, the shear strength improved by 42% at high temperatures compared with that of the Ti-28Ni material. Han et al[38] used Ti-50Ni to braze TZM alloys with ZrC_p-W composites, and the joints achieved a maximum shear strength of 146 MPa at room temperature when the brazing temperature was 1340 °C with a holding time of 10 min. This represents enhancement of 21% compared to the use of Ti-28Ni eutectic brazing material, while the shear strength at 800 °C remained unknown.

The fracture locations of the above Ti-Ni brazed joints were all located on the TZM side, as shown in Fig. 4a and 4b[34]. When the brazing temperature was 1000 °C, cracks are sprouted and expanded in the continuous Ti_2Ni layer, leading to joint fracture. The joints were characterized by intergranular fracture and transgranular fracture. With increasing the temperature, many Ti(s, s) streaks appear in the TZM matrix, as shown in Fig.4c and 4e. The fracture location moves to the TZM matrix, and the fracture is mainly due to the elongated grains parallel to the surface of hot-rolled TZM alloy. The brazing process causes the fracture by the streak Ti (s, s) solid solution formed by the intergranular infiltration, and the joints exhibit obvious brittle fracture characteristics. As shown in Fig.5[37], the schematic of the brazed joint formation process illustrates that when the temperature exceeds 993 °C, Ti-35Ni is melted and diffused into the substrate, resulting in appearance of lamellar microstructure in the TZM alloy substrate. The brazing materials penetrate the lamellar gap and react with the substrate to form a strip Ti-Mo solid solution. Initially, the WZ generates TiNi phase, as shown in Fig. 5d. As the brazing temperature decreases, Ti_2Ni phase ultimately forms, as depicted in Fig.5e and 5f. The continuous Ti_2Ni and Ti-Ni stripes form due to intergranular infiltration, which reduces the mechanical properties of the welded joint. To reduce joint brittleness, new elements were added to the original solders. For example, Cu can improve joint toughness and alleviate residual stress; Zr can promote the diffusion of elements at the joint, reducing MoO_2 segregation; Cr element in the same group as W and Mo, exhibits similar chemical properties, facilitating the bonding of elements in the joint.

In summary, future research directions include identifying optimal Ti-Ni ratio (Zr, Cr, Cu, etc), designing composite brazing structures, developing multilayer brazing materials, incorporating novel elements into brazing alloys, and exploring the implementation of diffusion barrier layers. There is a lack of effective theoretical models for the wetting and diffusion of brazing material, which requires more in-depth theoretical studies on brazing formation, as well as simulation of the forming process with the help of computers[59].

2.2 SPS diffusion bonding

SPS is a new method for diffusion joining of tungsten and

Table 1 Main research status of tungsten/molybdenum alloy welding technology[33–58]

Welding method	Welded joint	Shear strength/MPa	Tensile strength/MPa	Ref.
Brazing	TZM/Ni-44Ti/TZM	167	-	[33]
	TZM/Ni-13.7Ti/TZM	193		
	TZM/Ti-28Ni/ZrC_p-W	120.5 77.5 (800 °C)	-	[34–35]
	TZM/Ti-61Ni/ZrC_p-W	124.8 82.3 (800 °C)	-	[36]
	TZM/Ti-35Ni/ZrC_p-W	123.8 110.2 (800 °C)	-	[37]
	TZM/Ti-50Ni/ZrC_p-W	146	-	[38]
SPS diffusion bonding	TZM/WRe	498±32.5	475±19.8	[39]
	WRe/TZM	279.92	-	[40]
	ODS-W/TZM	-	485	[41]
	TZM/WRe	-	497±50	[42]
EBW	TZM/TZM (350 mm/min)	-	403	[43]
	TZM/TZM (370 mm/min)		364	
	TZM/TZM (390 mm/min)		256	
	Mo/Kovar (no offset)	-	190	[44]
	Mo/Kovar (offset 0.6 mm)		262	
	TZM/30CrMnSiA (beam current=24 mA)	-	191.3	[45]
	TZM/TZM	-	362	[46]
	TZM/Zr/TZM		452	
	TZM/TZM	-	362	[47]
	TZM/Re/TZM		524	
	TZM/30CrMnSiA	-	165.2	[48]
	TZM/V/30CrMnSiA		312.7	
LBW	NS-Mo/NS-Mo (3600 J/cm)	-	250	[49]
	NS-Mo/NS-Mo (250 J/cm)		570	
	Mo/Ti (offset 0.5 mm)	-	350	[50]
	Mo/301SS (offset 0.3 mm)	-	290	[51]
	La_2O_3-Mo/La_2O_3-Mo		617	[52]
	Mo-30W/Mo-30W	-	108.56	[53]
	Mo-30W/Ti/Mo-30W		409.57	
	Zr/Mo	-	76	[54]
	Zr/Ti/Mo		321	
	NS-Mo/NS-Mo	-	234	[55]
	NS-Mo/Zr/NS-Mo		441	
	La_2O_3-Mo/3Ti +1Zr/ La_2O_3-Mo	-	430	[56]
	Mo/304L	-	110	[57]
	Mo/Ni/304L		280	
	Mo/Ni (0.1 mm)/301SS	-	351	[58]

molybdenum alloys, utilizing strong pulsed direct current to generate Joule heat and to rapidly consolidate the powder[60–61]. As shown in Fig. 6a[39–40], columnar TZM and WRe alloy or powder were placed into a graphite mold, and specific upper and lower pressures were applied to the tungsten/molybdenum alloy. A temperature monitoring hole was set on the side to monitor the temperature. Diffusion welding is achieved through discharge activation, atomic diffusion and cooling[62–63]. Traditional sintering techniques such as hot pressing or hot isostatic pressing can obtain higher density, but the insulation time is too long and grain coarsening easily occurs, resulting in reduced mechanical properties. The characteristics

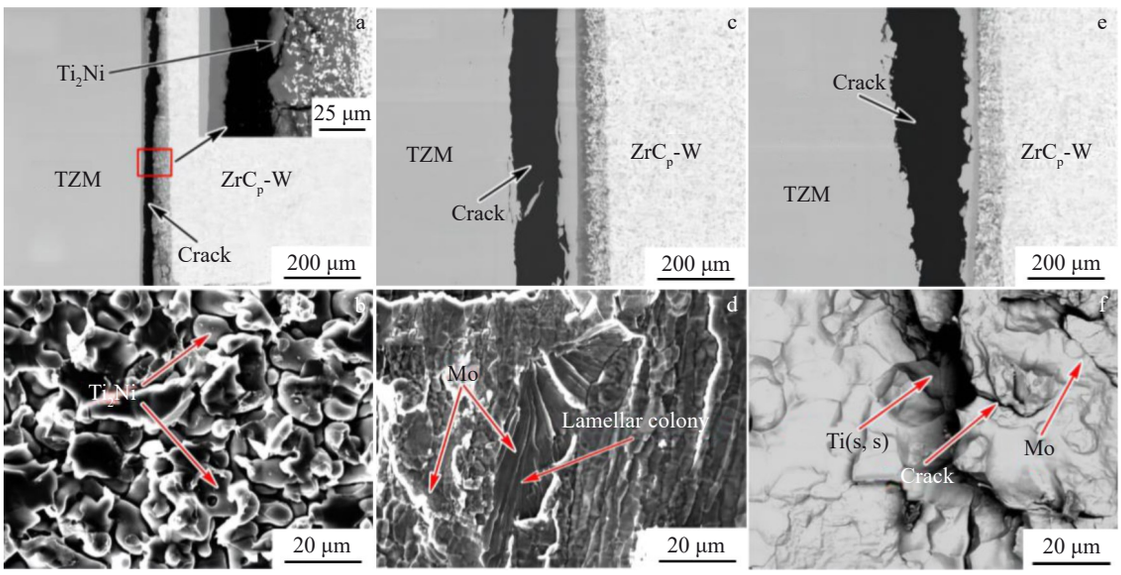

Fig.4 Cross-sectional BSE images of TZM/ZrC_p-W joints (a, c, e) and SEM images of corresponding fracture surfaces (b, d, f) at different brazing temperatures: (a–b) 1000 °C, (c–d) 1040 °C, and (e–f) 1080 °C [34]

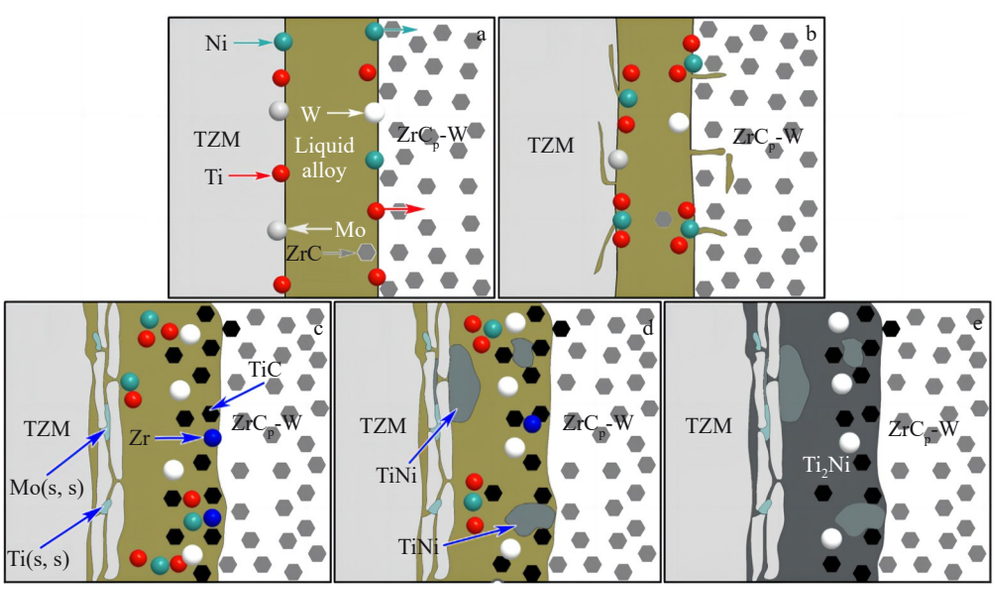

Fig.5 Melting of Ti-35Ni brazing material (a); diffusion of liquid TiNi alloy (b); formation of Ti-Mo solid solution and TiC (c); generation of TiNi (d); generation of Ti_2Ni (e)[37]

of rapid temperature rise sintering, high-pressure action, and low voltage and high current of SPS technique inhibit grain growth, thus accelerating densification, further controlling microstructure, and improving mechanical properties[64–65]. However, the main challenges of SPS diffusion welding lay in the precise control of temperature and holding time. Elevated temperatures can reduce porosity generation, but excessively high temperatures can induce coarse grains, and excessively long holding time can also result in grain coarsening and potential crack[66–67]. In the structure of the SPS sintering furnace, the accuracy of temperature measurement is questionable because the thermometer in the side temperature measurement hole is unable to penetrate deep into the furnace. Currently, SPS diffusion welding has gained applications in welding oxide dispersion strengthened tungsten-based materials (ODS-W) with TZM alloys and WRe/TZM alloys.

Liu et al[41] investigated the effective bonding of ODS-W alloy and TZM powder at different temperatures using SPS technique. Within the sintering temperature range of 1300–1600 °C, the metallurgical bonding at the interface was excellent, without defects such as intermetallic compounds, microcracks, or pores (Fig. 7)[41]. The highest tensile strength of 485 MPa was achieved at 1500 °C. The presence of Y_2O_3 particles at the interface increased the mutual diffusion

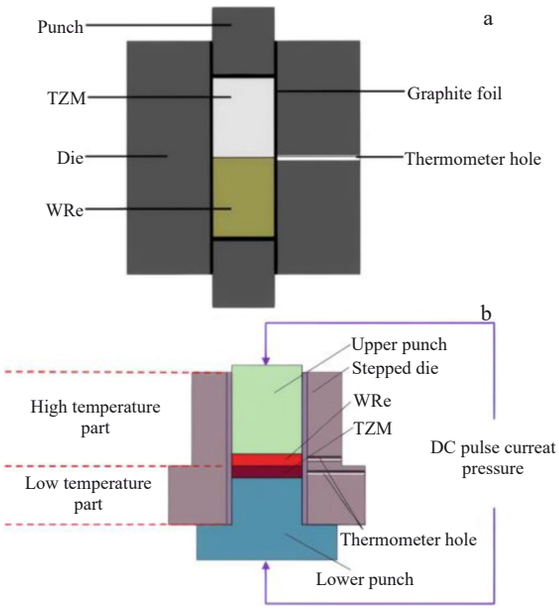

Fig.6 Schematic diagrams of traditional (a) and improved (b) graphite die-punch assembly during SPS-assisted diffusion welding[39–40]

distance between Mo and W, suggesting that Y_2O_3 particles could promote the diffusion between Mo and W and enhance joint strength. However, the mechanism of yttrium oxide particles enhancing joint strength is still unclear, and the causes of joint fracture remain uncertain. In particular, the impact of oxygen infiltration on the joints is not well understood. Further research can utilize transition state calculation methods in first-principles studies at the atomic level.

WRe/TZM alloy welded joints are often used as CT scanner X-ray targets, where the tungsten alloy serves as the anode target surface material, bombarded by an electron beam to produce X-rays, and TZM alloy serves as the dielectric disk between the target surface and heat dissipating portion[68]. TZM alloy not only exhibits excellent thermal conductivity and high-temperature performance, but its density is also only half of that of WRe alloy, and its specific heat capacity is more than twice that of WRe alloy. Therefore, by welding and combining the WRe alloy and TZM alloy, the mass of the target plate can be significantly reduced, and rapid heat dissipation of the target plate can be achieved, thereby extending the service life of the target plate[69].

Yang et al[39] employed the SPS technique to achieve solid-state diffusion bonding between TZM alloy and WRe alloy in the sintering temperature range of 1300–1600 °C for 30 min. The results reveal that the joints are bonded within the range of 1300–1600 °C, incomplete bonding is observed at 1300 °C and plastic deformation occurs at 1600 °C. The WRe/TZM alloy joints exhibit the highest quality, which are free of cracks and porosity, and after holding at 1500 °C for 30 min, it possesses shear strength of 498±32.5 MPa and tensile strength of 475±19.8 MPa. Fracture morphology exhibits a mixed pattern of through-crystal disintegration and along-crystal fracture. Similar conclusions are drawn by Hu et al[42]. In the thermal shock performance evaluation test, TZM/WRe joints (1500 °C/30 min) did not crack and maintained high strength after 1500 times repetitive thermal shocks. Harimon et al[70] demonstrated that the fatigue strength of laminated WRe/TZM specimens surpasses that of bulk WRe alloy specimens. Therefore, in practical application of CT scanner X-ray targets, the structure can be enhanced by laminated WRe/TZM.

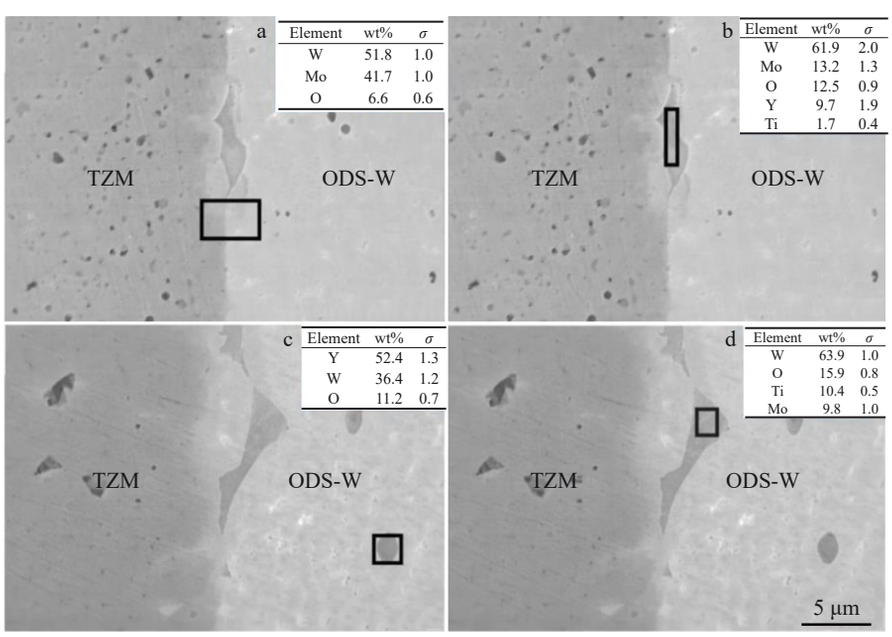

Fig.7 SEM images and EDS point-scan results of ODS-W/TZM alloy joints at different temperatures: (a) 1300 °C, (b) 1400 °C, (c) 1500 °C, and (d) 1600 °C[41]

Han et al[40] investigated a novel mold with a stepped structure for sintering WRe and TZM alloy powders, and used two temperature monitoring holes to measure the temperatures of WRe and TZM alloys. As shown in Fig. 6b, the structure has different temperatures at locations of two alloys, with a maximum temperature difference of approximately 190 °C. The gradient mold, which establishes different sintering temperatures, allows simultaneous densification and bonding of WRe and TZM alloy powders, resulting in superior microstructure and mechanical properties. The highest shear strength of the joint was 279.92 MPa (T=1600 °C, t=8 min, P= 30 MPa). The high mechanical properties are fundamentally determined by microstructural characteristics such as relative density, grain size and morphology. The primary factor influencing these characteristics is temperature; excessively high temperatures and prolonging holding time can lead to grain growth, reduce densification, and promote formation of new defects such as microcracks. The gradient structure enables the production of joints with excellent relative density, grain size, and morphology through one-step sintering of the powders, offering a new approach for producing X-ray targets for CT scanners.

2.3 EBW

EBW of tungsten/molybdenum alloys, as a high-end welding technique, has the advantages of high energy density, fast welding speed, and small HAZ[71]. Molybdenum alloys are sensitive to oxygen content and heat source energy density in welding, and EBW is one of the most suitable fusion welding methods used to join molybdenum alloys, considering vacuum atmosphere protection and high energy density[25]. However, high heat input of EBW makes the joints susceptible to grain coarsening, and coarse grains will lead to increase in brittleness of the welded joints and decrease in mechanical properties, as well as cracks and porosity[72–73]. In view of the above problems, measures such as adjusting welding parameters and adding suitable intermediate layer metals may be adopted to improve the quality of welded joints in order to ensure the reliability and stability of welding.

2.3.1 Welding parameters

The main welding parameters that affect the quality of tungsten/molybdenum alloy EBW joints include welding speed, beam offset position and beam current size. Different welding parameters can affect the welding efficiency and the distribution of precipitates, alter the morphology of the reaction layer, and lead to different mechanical properties[74–75].

Wang et al[43] investigated the effect of welding speed on microstructure and mechanical properties of vacuum EBWed TZM alloy joints. It is observed that an increase in welding speed reduces the size of the grains but exacerbate the segregation of MoO_2 particles on the grain boundaries, resulting in stress concentration and reduction in the tensile strength of the weld, and leading to severe intergranular fracture. The tensile strength of the welded joint was 403 MPa when the welding speed was 350 mm/min, whereas it decreased to only 256 MPa when the welding speed was 390 mm/min. Chen et al[44] studied the effect of electron beam offset on the microstructure and mechanical properties of welded molybdenum and Kovar alloy joints. When the beam was not offset, WZ consisted of columnar crystals, and the tensile strength was only 190 MPa. However, when the beam was offset to the Kovar alloy by 0.6 mm, the weld mainly comprised equiaxial crystals, and tensile strength of welded joint increased to 262 MPa, improved by 37.9% compared to that of the no-beam offset condition. Beam deflection prevents the formation of voids and gaps on the Mo-side fusion line, yet the issue of joint embrittlement remains unresolved, so the next work should focus on finding an intermediate layer with better compatibility with the substrate to prevent the emergence of brittle phases. Wang et al[45] conducted EBW tests on TZM alloy and 30CrMnSiA steel using different electron beam currents. As the beam current increased, the thickness of the Fe_2Mo reaction layer decreased. At a beam current of 24 mA, the joint strength peaked at 191.3 MPa, and fractures occurred along the Fe_2Mo layer near the TZM alloy side, exhibiting a brittle fracture mode. However, the formation mechanism of the reaction phase in the center of the weld remained unclear, and the reasons for the formation of porosity in the joint were not extensively explained.

2.3.2 Different intermediate layer metals

Controlling the energy distribution by adjusting the electron beam current and the electron beam offset distance can optimize the mechanical properties of the joints. However, the improvement is not significant, primarily because the embrittlement of the joints is not fundamentally resolved. The reliability of the joints can be enhanced by employing lowmelting-point filler materials. The addition of a suitable intermediate layer can prevent the formation of MoO_2, furthering improving the grain structure, increasing the strength and toughness of the welded joints, and altering the fracture mode. The intermediate layer used to regulate the EBWed joints of TZM alloys is typically based on Zr, Re and V.

Wang et al[46] used Zr as interlayer to analyze the structure of EBWed joints of TZM alloy. As depicted in Fig. 8[46], joints lacking pure zirconium foil as an interlayer exhibit MoO_2 and TiO_2 precipitation at the grain boundaries. Upon the addition of zirconium as interlayer, MoO_2 and TiO_2 precipitation at the grain boundaries are ceased in the welded joints, and a multitude of second-phase particles, mainly ZrO_2, are precipitated within the grain, which leads to increase in the tensile strength of the joints to 452 MPa. Although the tensile strength of the joint is improved, fracture still occurs in the WZ, demonstrating a fully transgranular cleavage fracture mode. To further enhance the joint strength, Zhang et al[47] conducted EBW tests on TZM alloys with varying thicknesses of Re as the intermediate layer. The weld area of different joints was measured using Image Pro Plus. When the Re content in the WZ was 48.7%, the tensile strength of the joint reached 524 MPa, and the fracture location shifted from the WZ to the HAZ.

Yu et al[48] opted pure vanadium as filler metal for EBW of TZM/30CrMnSiA. The tensile strength of the joints was only

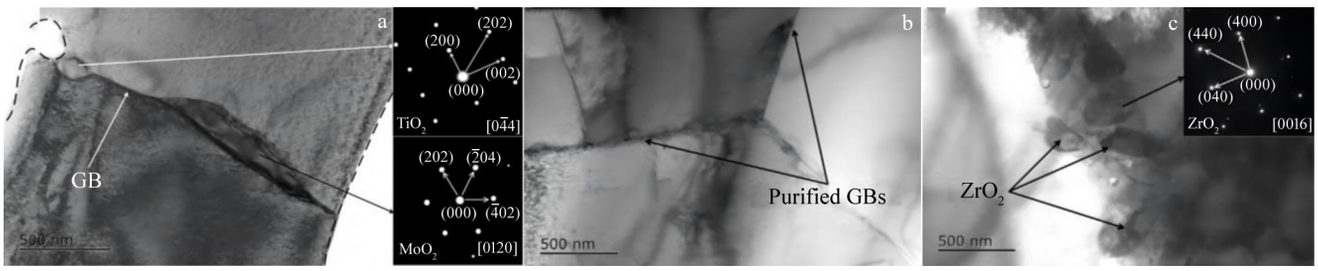

Fig.8 TEM micrographs of welded joints: (a) without adding zirconium; (b) purification of GBs region in joints after addition of zirconium; (c) ZrO_2 particles distributed within the grains[46]

165.2 MPa without V-foil filler and 312.7 MPa with V-foil, indicating that the metallurgical modulation of the alloy by pure V-foil is significant. The joints fractured in the HAZ on the TZM side. First-principle calculations show that for the Mo (111)/Fe_2Mo (100) interface, there are more charge vacancies at the interface, whereas for the Mo (111)/V(Fe)ss(111) interface, the charge density is high, resulting in the formation of strong chemical bond, and the interfacial work of adhesion is higher, thus providing better mechanical properties, as illustrated in Fig.9[48].

2.4 LBW

LBW technique for tungsten/molybdenum alloys is highly regarded for high energy density, precise control of heating position and heat input, narrow fusion zone and low residual stress[76]. However, it faces issues related to undesirable microstructure and degraded mechanical properties, such as high porosity and brittle compounds. To address these problems, welding parameters are adjusted, and suitable intermediate layer metals are added to achieve high-quality joints with improved mechanical properties.

2.4.1 Welding parameters

Similar to EBW, adjusting LBW parameters, including heat input, beam offset and interface gap, can regulate the microstructure of the tungsten/molybdenum alloy laser welded interface. This control enables grain refinement, reduces porosity, suppresses segregation and defect formation, and ultimately improves the mechanical properties and quality of the joints.

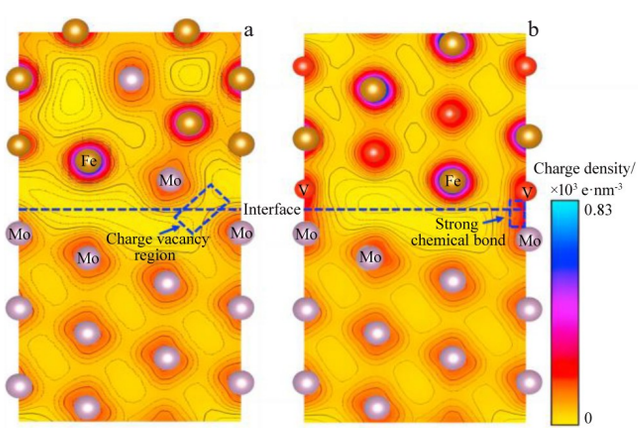

Fig.9 Charge density at Mo (111)/Fe_2Mo (100) interface (a) and Mo (111)/V(Fe)ss (111) interface (b)[48]

Xie et al[49] investigated the low heat input laser welding of nanostructured high-performance molybdenum alloy (NS-Mo) joints. They found that when the welding heat input was reduced from 3600 J/cm to 250 J/cm, the low heat input and high welding speed significantly refined the grains in the FZ of the joints, decreased the degree of MoO_2 segregation, and markedly reduced the number of porosity defects (Fig.10)[49]. The porosity decreased from 10.7% to 2.1%, and the tensile strength of the welded joints increased from 250 MPa to 570 MPa. Low heat input welding improved the strength of the welded joints by refining the grains and increasing the total grain boundary area, thereby reducing the degree of MoO_2 segregation at the grain boundaries. Porosity decreased from 10.7% to 2.1%, and the tensile strength of welded joints increased from about 250 MPa to 570 MPa. Low heat input welding improved the strength of welded joints by reducing the degree of MoO_2 segregation at grain boundaries through grain refinement and increasing the total area of grain boundaries. Zhang et al[50] studied the effect of beam offset on the laser welding of molybdenum and titanium. They found that porosity at the joint decreases with increasing the beam offset. When the laser was offset by 0.5 mm towards the titanium, the maximum tensile strength was approximately 350 MPa, which was about 70% of that of the titanium substrate. The HAZ of molybdenum and the interface between the molybdenum plate and the HAZ are identified as the weakest regions of the Mo/Ti joint, suggesting that strengthening HAZ can be a direction for future research. Gao et al[51] investigated the effect of laser offset on the microstructure and mechanical properties of LBW of pure molybdenum and stainless steel. They observed that when the laser beam was shifted from the molybdenum side to the stainless-steel side by 0.2 – 0.3 mm, the reduced amount of molten molybdenum effectively suppressed weld defects and the formation of Fe-Mo intermetallic compounds. However, when the laser offset exceeded 0.4 mm, incomplete fusion occurred at the Mo/Fe interface due to poor wetting and diffusion of Mo by the 301SS melt. The maximum tensile strength of the joint was 290 MPa with 0.3 mm offset. Regardless of the laser beam offset position, all welded joints fractured in the FZ layer, exhibiting a brittle fracture mode.

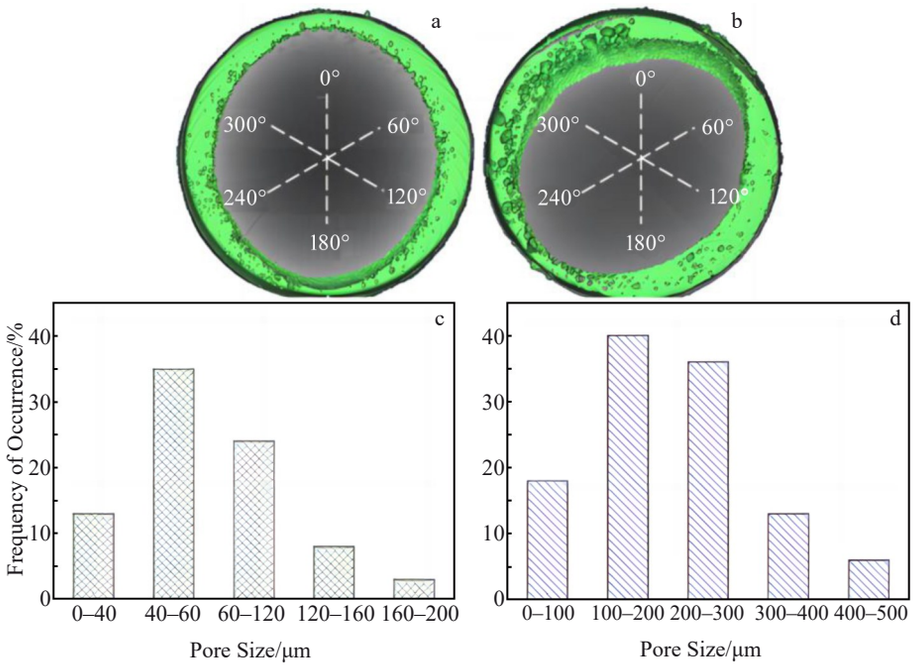

Fig.10 CT test (a – b) and statistical results (c – d) of porosity distribution of laser welded NS-Mo alloy joints at different heat inputs: (a, c) 250 J/cm and (b, d) 3600 J/cm[49]

Ning et al[77] investigated the effect of interfacial gap on joint porosity and embrittlement in laser lap welding of TZM alloy. Porosity and embrittlement were identified as the primary factors reducing the strength and ductility of welded joints. They found that a 0.09 mm interfacial gap can reduce porosity to 3%, and the tensile strength of the welded joints can reach approximately 60% of that of the BM. An et al[52] conducted a series of experiments on La_2O_3 dispersion-strengthened molybdenum alloy by laser lap welding and analyzed the effects of laser power, defocus distance and welding speed on the tensile strength of the laser-welded joints. The tensile strength of the joints reached 617 MPa under optimal conditions (P=2500 W, f =1 mm and v=6 m/min), which was 82.3% of that of the BM. During tensile testing, the joints exhibited almost no plastic deformation and underwent brittle fracture, likely due to oxygen-induced embrittlement. Future research should focus on adding a suitable intermediate layer to reduce oxygen content.

2.4.2 Different intermediate layer metals

The addition of Ti, Zr and Ni interlayers plays an important role in modulating the tungsten/molybdenum alloy weld interface in LBW. This includes inhibiting phase transformations, reducing brittle phase formation, counteracting the weakening of joint strength by oxygen, modulating grain boundary structure, enhancing tensile strength, and influencing fracture mode.

Cheng et al[53] investigated the effect of Ti interlayer on the microstructure and properties of Mo-30W alloy laser welded joints. After the addition of Ti element, the impurity element O could react with Ti to mainly form the TiO_2 phase, which had almost no effect on Mo grain boundary strength relative to Mo. Comparing the Gibbs free energy of the second phases TiO_2, MoO_2 and WO_2, TiO_2 with lower energy was more likely to be generated, thus reducing the formation of MoO_2 and WO_2 that were not conducive to the strength of the grain boundary[78]. The tensile strength of the joints increased from 108.56 MPa to 409.57 MPa, showing a 270% increment. Zhang et al[54] added 1 mm pure Ti as an intermediate layer in Zr/Mo LBW, which effectively prevented the brittle Mo_2Zr phase from being generated in the transition layer at the Mo-FZ interface. The tensile strength of the joints increased from 76 MPa to 321 MPa compared to the joints without adding Ti as an intermediate layer. Additionally, Zhang et al[55] chose zirconium as filler material for LBW of molybdenum alloys and found that ZrO_2 preferentially formed inside the grains, mitigating the segregation of MoO_2. The tensile strength of the welded joints increased from 234 MPa (without Zr) to 441 MPa (with 0.05 mm of Zr as the intermediate layer), and the fracture mechanism changed from intergranular fracture to deconvoluted fracture. Further study may focus on the effect of Ti and Zr content on laser welded molybdenum alloy joints.

Zhang et al[56] investigated the laser welding of La_2O_3-Mo using different combinations of Ti foil (0.04 mm) and Zr foil (0.03 mm) as intermediate layers. Zr provides second-phase strengthening, and Ti contributes to solid solution strengthening[79]. By incorporating different mass ratios of Ti and Zr, the relative content of Mo_2Zr phase and solid solution atoms in the fusion zone can be controlled. The joint with 3Ti+1Zr intermediate layer achieved a tensile strength of 430 MPa and a hardness of 3676.96 MPa, balancing strength and ductility.

Zhang et al[57] studied the effect of adding Ni to laser-welded Mo/304L joints, and found that at the optimal offset, the tensile strength of the joint increased from 110 MPa to 280 MPa, as shown by electron probe X-ray microanalysis

(EPMA) in Fig.11[57]. Ni improved the diffusion ability of Mo, increasing the diffusion distance of the Mo element at the Mo/FZ interface from 7.4 μm to 9.7 μm. Fractures mainly occurred near the Mo/FZ interface, exhibiting intergranular fracture. The reaction mechanism of the elements at the center of the joint remained unclear, and the addition of Ni complicated the joint mechanism. Notably, the FZ/304L interface is not a weak part of the joint, warranting further in-depth analysis. To determine the most suitable Ni interlayer thickness for Mo and steel joints, Gao et al[58] investigated three thicknesses of the Ni interlayer (0.05, 0.10 and 0.20 mm) and found that the tensile strength was maximized at 351 MPa with a thickness of 0.10 mm. However, further increasing the thickness to 0.20 mm resulted in incomplete fusion, voids and cracks, leading to gradual deterioration in the mechanical properties of the welds.

3 Effect of Tungsten/Molybdenum Alloy Doping Treatment on Welding

Doping and alloying design not only improves the high-temperature strength, low-temperature plasticity and oxidation resistance of molybdenum and tungsten, but also plays an important role in enhancing the quality of tungsten/molybdenum alloy welded joints[80–81]. Rare earth oxides such as La_2O_3, Al_2O_3 and Y_2O_3 particles were added[82–84], along with simultaneous doping of titanium, zirconium, silicon and metal carbide TiC and ZrC particles[85–86], to achieve a uniform grain structure, inhibit grain coarsening at high temperatures, and reduce porosity[87]. The doped elements in the weld not only have solid-solution strengthening and diffuse strengthening effects but also promote element diffusion, thereby improving the plasticity and tensile strength of welded joints[88–89].

3.1 Doped oxides

In the previous sections, SPS diffusion welding of ODS-W/TZM, doped with Y_2O_3 particles, can promote the diffusion of elements at the joint, thereby enhancing the mechanical properties of the joint. La_2O_3-Mo alloy laser lap welding under different welding parameters yielded good mechanical properties of the joints[52], but the mechanism of tungsten/molybdenum alloy joints strengthened by the dispersion of rare-earth oxides was not explained in detail. The key to improving the performance of tungsten/molybdenum alloy welded joints lay in suppressing grain coarsening and porosity defects at high temperatures, and doping dispersed fine-crystalline rare-earth oxides can refine the grains, fill the pores, and improve the strength and toughness of tungsten/molybdenum alloys[90].

Wang et al[91] investigated the microstructural properties of La_2O_3-doped tungsten-based materials and found that the densification mechanism was mainly the filling of pores by La_2O_3 particles. Min et al[92] compared Y_2O_3-doped tungsten with pure tungsten, revealing that a large number of pores existed at grain boundaries and grain triple junctions of pure W (Fig. 12a and 12c)[92], whereas the W-Y fracture exhibited almost pores. Tens of nanometer-sized second-phase particles were observed at the grain triple junctions of W-Y (Fig. 12b and 12d), aiding in fixing the grain boundaries and thus refining the grains of W-Y. Lan et al[93] investigated the effects of rare earth oxides Y_2O_3, CeO_2 and La_2O_3 on the sintering performance, microstructure and mechanical properties of Mo-W solid solution alloys. These three oxides exhibited similar capabilities in inhibiting grain growth and promoting grain refinement, and La_2O_3 doping was the most beneficial for achieving a dense and fine-grained Mo-W solid solution alloy[94]. Future research directions can focus on exploring the effects of other rare earth oxides and carbides (such as NbC and HfC) on the strengthening mechanisms and mechanical properties of welded joints[95].

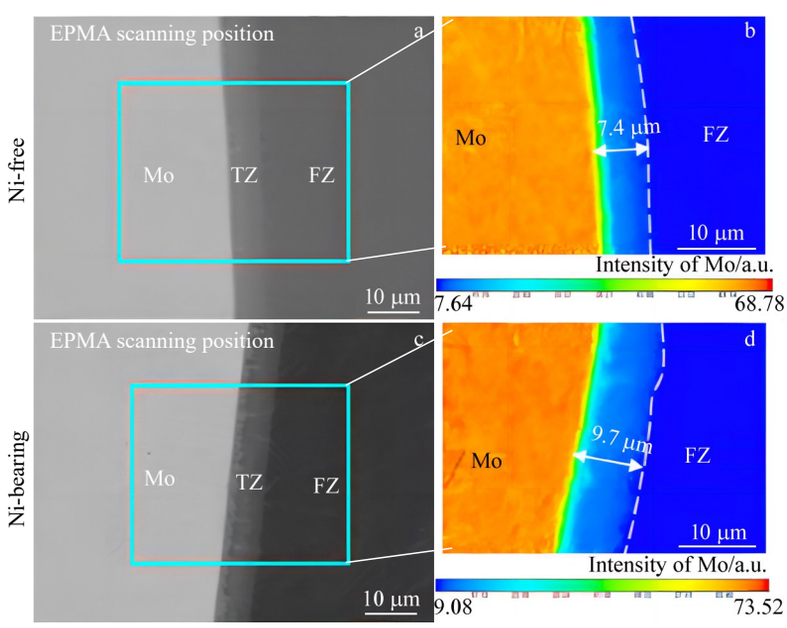

Fig.11 EPMA results for molybdenum/SUS304L laser welded Ni-free (a–b) and Ni-bearing (c–d) joints[57]

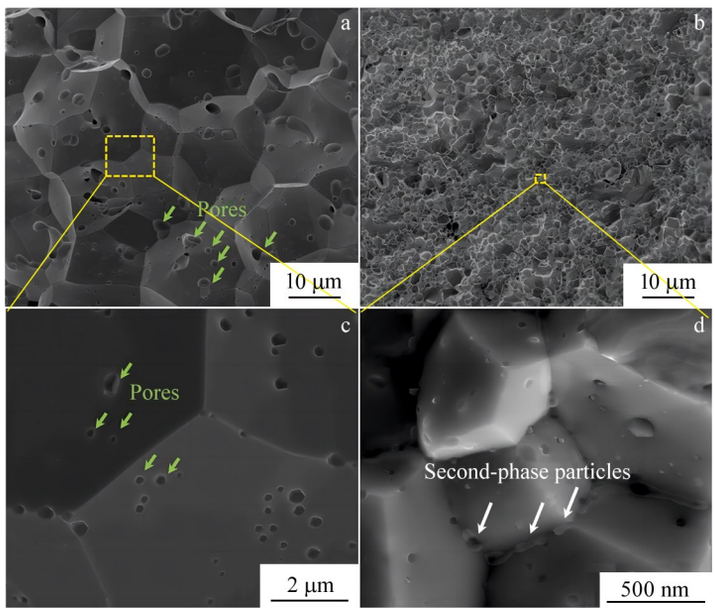

Fig.12 Fracture surface images of pure W (a, c) and W-Y alloys (b, d) after SPS sintering and disruption[92]

3.2 Doped carbons

Compared with oxide diffusion strengthening, doping TiC, ZrC or other carbide particles can effectively inhibit grain growth and grain boundary migration of the molybdenum matrix, resulting in a uniform grain structure and excellent high-temperature strength and toughness[96–97]. The strengthening mechanism of carbide-doped ZrCp/W composites involves grain refinement of tungsten and load transfer from the tungsten matrix to hard ZrC particles, although excessively high ZrC content leads to increased porosity[98]. The uniformity and fineness of doped carbides are crucial for strengthening molybdenum alloys, as uneven carbide distribution tends to cause agglomeration during sintering[99–100]. Hu et al[101] studied the refinement of Mo alloy grains by TiC particles, and reduced the composite powder size of Mo grains from 302 nm to 95 nm. The investigation of ultra-fine grains aims to enhance the diffuse reinforcement effect on tungsten and molybdenum alloy matrices, facilitating the resolution of grain coarsening issues at high temperatures in tungsten/molybdenum alloy welding. This, in turn, improves the mechanical properties of the joints, expanding their application in high-temperature fields[102–103].

3.3 Other elements

Zhang et al[104] investigated the strengthening mechanism of carbon and titanium combined alloying in molybdenum alloy laser welded joints. They carburized the Mo alloy plate and used Ti foil as the interlayer for LBW. The maximum tensile strength of the joints was 406.6 MPa, whereas the tensile strength of pure Mo joints was only 100 MPa. Ref. [105] explored the effect of Si and Ti combined alloying on the microstructure and properties of molybdenum laser welded joints. It is found that the tensile strength of the joints was 231.6 MPa with Si powder and Ti powder in a mass ratio of 1:1 as the intermediate layers. Moreover, when Mo alloy plate or sleeve was used as the BM for LBW, the tensile strength of the joints reached 301 MPa. Combined alloying significantly reduced the cracks caused by stress concentration at the FZ and ensured the strength of the HAZ while improving the strength of the FZ, providing a new idea for the strengthening of molybdenum fusion welded joints.

4 Research Shortcomings and Prospects

Tungsten/molybdenum alloy welding is considered beneficial for structural lightweighting and cost reduction, offering broad application prospects. However, it still faces unresolved issues, such as joint brittleness, porosity, unknown mechanism and weak strength in the HAZ. Introducing new welding methods or combinations of welding techniques, as well as the utilization of modern analytical techniques, such as computer simulation, artificial intelligence and machine learning, is essential for conducting more in-depth and comprehensive studies on the effects of welding process on microstructure and mechanical properties of welded joints. This approach aims to achieve highly efficient and high-quality welding production.

4.1 Problems

During the brazing of TZM and ZrC_p-W alloys, brittle compounds tend to form at the welded joint, and intergranular penetration in the molybdenum alloy matrix may lead to cracks, thereby reducing the toughness and strength of the welded joint. Current research primarily focuses on the Ti-Ni filler metal ratio or evaluating the interfacial microstructure and bonding performance of the brazed joints through a series of conventional temperature tests and characterization methods. However, microstructural control remains suboptimal, and the impact of intergranular penetration on the joint has not been resolved. The region near the brazing seam in the TZM alloy matrix is identified as the weakest part of the joint.

The main challenge in the SPS diffusion bonding of tungsten alloy and molybdenum alloy is the precision control of temperature and the accuracy of temperature measurement. Increasing the temperature can reduce the generation of porosity, but excessively high temperatures or long holding time will result in grain coarsening and cracking, posing difficulties in accurately controlling the microstructure. Additionally, the shape and modeling requirements of materials for SPS diffusion bonding are relatively high. The sintering method (furnace size and pressurization method) determines that large and complex structures of welded parts are challenging to achieve.

The main challenge in EBW and LBW of tungsten alloy and molybdenum alloy are grain coarsening caused by high energy input, segregation of MoO_2 particles and stress concentration at grain boundaries. Selecting suitable intermediate layer materials, controlling welding parameters, and optimizing the welding process can inhibit cracks, porosity and the generation of intermetallic compounds. Many existing studies lack systematic research and theoretical guidance for the corresponding relationship between welding parameters and intermediate layer matching.

The study of tungsten/molybdenum alloy doping mainly focuses on the addition of La_2O_3, Al_2O_3, ZrO_2 and Y_2O_3 particles, as well as metal carbide TiC and ZrC particles. However, excessively high doping content is prone to agglomeration, leading to increased porosity and cracks. How to obtain uniform doping and add an appropriate amount of doping to achieve high-temperature mechanical properties of the joints, as well as their microstructural features and strengthening effects, is rarely reported.

4.2 Outlooks

1) Research on brazing tungsten/molybdenum alloys should broaden the scope of brazing materials to develop new, excellent brazing alloys beyond the Ti-Ni base for tungsten/molybdenum alloy brazing. Additionally, incorporating new elements (Zr, Cr, Cu, etc) and implementing diffusion barrier layers can further strengthen the HAZ region on the molybdenum side, achieving joints with superior mechanical properties.

2) In terms of SPS diffusion welding of tungsten and molybdenum alloys, future research should focus on two main aspects. Firstly, optimizing the welding process through more advanced temperature control and testing systems enable more precise control of the microstructure, thus ensuring densification and grain refinement during the welding process. Secondly, improving the equipment pressure application method allows welding of complex structural components.

3) Further research on EBW and LBW of tungsten/molybdenum alloys should focus on grain refinement and the inhibition of brittle compound formation. A comprehensive review of the welding process, including welding parameters and interlayers, is necessary. Additionally, appropriate preheating and post-heating techniques combined with doping and composite alloying methods can enhance the strength of the FZ region while ensuring the strength of the HAZ region.

References

1 Wei Y N, Li H, Peng X *et al. International Journal of Refractory Metals and Hard Materials*[J], 2020, 92: 105287

2 Meng X C, Li L, Li C L *et al. Corrosion Science*[J], 2022, 200: 110202

3 Webb J, Gollapudi S, Charit I. *International Journal of Refractory Metals and Hard Materials*[J], 2019, 82: 69

4 Chen Q Y, Liang S H, Li B X *et al. International Journal of Refractory Metals and Hard Materials*[J], 2021, 100: 105668

5 Kumar M, Gurao N P, Upadhyaya A. *International Journal of Refractory Metals and Hard Materials*[J], 2022, 105: 105849

6 De Prado J, Sánchez M, Ureña A. *Journal of Nuclear Materials*[J], 2017, 490: 188

7 Gardia D K, Khan A R, Patra A. *Materials Today: Proceedings*[J], 2022, 62: 6204

8 Cwalina K L, Demarest C R, Gerard A Y *et al. Current Opinion in Solid State and Materials Science*[J], 2019, 23(3): 129

9 De Prado J, Sánchez M, Ureña A. *Materials & Design*[J], 2016, 99: 93

10 Zhang L L, Zhang L J, Ning J *et al. Journal of Materials Processing Technology*[J], 2021, 296: 117184

11 Peng S X, Mao Y W, Min M *et al. International Journal of Refractory Metals and Hard Materials*[J], 2019, 79: 31

12 Duport M, Lhuisser P, Blandin J J *et al. Additive Manufacturing*[J], 2023, 61: 103340

13 Averchenko A V, Salimon I A, Zharkova E V *et al. Materials Today Advances*[J], 2023, 17: 100351

14 Miškovičová J, Anguš M, Van der Meiden H *et al. Fusion Engineering and Design*[J], 2020, 153: 111488

15 Burkov A A, Chigrin P G. *Surface and Coatings Technology*[J], 2018, 351: 68

16 Senthilnathan N, Annamalai A R, Venkatachalam G. *Materials Science and Engineering A*[J], 2018, 710: 66

17 Tuzemen C, Yavas B, Akin I *et al. Journal of Alloys and Compounds*[J], 2019, 781: 433

18 Hu W Q, He J, Yang Z W *et al. Materials Characterization*[J], 2023, 203: 113063

19 Xie M X, Li Y X, Shang X T *et al. Metals*[J], 2019, 9(6): 640

20 Leitner K, Lutz D, Knabl W *et al. Scripta Materialia*[J], 2018, 156: 60

21 Zhang L L, Zhang L J, Long J *et al. Materials & Design*[J], 2019, 181: 107957

22 Talignani A, Seede R, Whitt A *et al. Additive Manufacturing*[J], 2022, 58: 103009

23 Wang Z M, Qin J Y, Hu Q *et al. Journal of Membrane Science*[J], 2020, 608: 118200

24 Dong G Y, You X G, Dong L Y *et al. Journal of Materials Research and Technology*[J], 2022, 20: 4297

25 Zhang Y Y, Wang T, Jiang S Y *et al. Materials Science and Engineering A*[J], 2017, 700: 512

26 Wang D Z, Yu C F, Ma J *et al. Materials & Design*[J], 2017, 129: 44

27 Zhang L J, Liu J Z, Pei J Y *et al. Journal of Manufacturing Processes*[J], 2019, 41: 197

28 Wang J, Xiong Q L, Wang J *et al. Vacuum*[J], 2019, 169: 108942

29 Lu Shenghui, Zheng Jianping, Qi Lijun *et al. Rare Metal Materials and Engineering*[J], 2020, 49(6): 2054 (in Chinese)

30 Han G H, Zhao H Y, Fu W *et al. Transactions of the China Welding Institution*[J], 2017, 38(1): 69

31 Lu Q B, Long W M, Zhong S J *et al. Welding in the World*[J], 2020, 64: 1877

32 Lu Q B, Zhong S J, Li S G *et al. Rare Metal Materials and Engineering*[J], 2020, 49(3): 849

33 Lu Q B, Zhong S J, Li S N *et al. Rare Metal Materials and Engineering*[J], 2019, 48(8): 2418

34 Han G H, Wang Y F, Zhao H Y *et al. International Journal of Refractory Metals and Hard Materials*[J], 2017, 69: 240

35 Tian Xiao, Zhao Hongyun, Song Xiaoguo *et al. Rare Metal Materials and Engineering*[J], 2018, 47(3): 927 (in Chinese)

36 Han G H, Bian H, Zhao H Y *et al. Journal of Alloys and Compounds*[J], 2018, 747: 266

37 Song X G, Han G H, Hu S P *et al. Materials Science and Engineering A*[J], 2019, 742: 190

38 Han Guihai, Zhao Hongyun, Song Xiaoguo *et al. Rare Metal Materials and Engineering*[J], 2018, 47(6): 1936 (in Chinese)

39 Yang Z, Hu K, Hu D W *et al. Journal of Alloys and Compounds*[J], 2018, 764: 582

40 Han C L, Yang X Y, Nong B R *et al. Journal of Materials Research and Technology*[J], 2021, 15: 2646

41 Liu D G, Ma H R, Ruan C F *et al. Results in Materials*[J], 2021, 9: 100175

42 Hu Dawei, Yang Zhi, Xu Ke *et al. Transactions of the China Welding Institution*[J], 2018, 39(11): 73 (in Chinese)

43 Wang T, Li N, Zhang Y *et al. Vacuum* [J], 2018, 149: 29

44 Chen G, Yin Q, Guo C *et al. Journal of Materials Processing Technology*[J], 2019, 267: 280

45 Wang T, Yu B, Wang Y F *et al. Chinese Journal of Aeronautics*[J], 2021, 34(8): 122

46 Wang T, Zhang Y Y, Jiang S Y *et al. Journal of Materials Processing Technology*[J], 2018, 251: 168

47 Zhang Y Y, Wang T, Jiang S J *et al. Journal of Manufacturing Processes*[J], 2018, 32: 337

48 Yu B, Wang T, Lv Y Z *et al. Materials Science and Engineering A*[J], 2021, 817: 141369

49 Xie M X, Li Y X, Shang X T *et al. Materials*[J], 2019, 12(9): 1433

50 Zhang L J, Lu G F, Ning J *et al. Materials*[J], 2018, 11(10): 1852

51 Gao X L, Li L K, Liu J *et al. International Journal of Refractory Metals and Hard Materials*[J], 2020, 88: 105186

52 An G, Sun J, Sun Y *et al. Materials*[J], 2018, 11(7): 1071

53 Cheng P X, Zhang L J, Ning J *et al. Journal of Materials Engineering and Performance*[J], 2022, 31(10): 8542

54 Zhang L J, Ma R Y, Zhang Y B *et al. Optics & Laser Technology*[J], 2020, 131: 106327

55 Zhang L J, Pei J Y, Zhang L L *et al. Journal of Materials Processing Technology*[J], 2019, 267: 338

56 Zhang L L, Zhang L J, Ning J *et al. International Journal of Refractory Metals and Hard Materials*[J], 2021, 101: 105662

57 Zhang L J, Wang C H, Zhang Y B *et al. Materials & Design*[J], 2019, 182: 108002

58 Gao X L, Li L K, Liu J *et al. International Journal of Refractory Metals and Hard Materials*[J], 2021, 100: 105654

59 De Prado J, Sánchez M, Utrilla M V *et al. Materials & Design*[J], 2016, 112: 117

60 Gaffin N D, Ang C, Milner J L *et al. International Journal of Refractory Metals and Hard Materials*[J], 2022, 104: 105778

61 Hu K, Li X Q, Guan M *et al. International Journal of Refractory Metals and Hard Materials*[J], 2016, 58: 117

62 Wang Yueming, Tang Qiuhao, Xiong Xiang. *Rare Metal Materials and Engineering*[J], 2021, 50(3): 1044 (in Chinese)

63 Rao Mei, Luo Guoqiang, Zhang Jian *et al. Rare Metal Materials and Engineering*[J], 2018, 47(11): 3536 (in Chinese)

64 Danisman C B, Yavas B, Yucel O *et al. Journal of Alloys and Compounds*[J], 2016, 685: 860

65 Ding L, Xiang D P, Pan Y L *et al. Journal of Alloys and Compounds*[J], 2017, 712: 593

66 Jasper B, Schoenen S, Du J *et al. Nuclear Materials and Energy*[J], 2016, 9: 416

67 Annamalai A R, Muthuchamy A, Srikanth M *et al. Materials*[J], 2021, 14(19): 5756

68 Yavas B, Goller G. *International Journal of Refractory Metals and Hard Materials*[J], 2019, 78: 273

69 Hao Y P, Tan C W, Yu X D *et al. Journal of Alloys and Compounds*[J], 2020, 819: 152975

70 Harimon M A, Miyashita Y, Otsuka Y *et al. Materials & Design*[J], 2018, 137: 335

71 Yin Q X, Chen G Q, Ma Y R *et al. Materials Science and Engineering A*[J], 2022, 851: 143619

72 Chen G Q, Liu J P, Shu X *et al. Vacuum*[J], 2018, 154: 1

73 Zi P F, Li L, Cao L *et al. Rare Metal Materials and Engineering*[J], 2019, 48(8): 2413

74 Yeganeh V E, Li P. *Materials & Design*[J], 2017, 124: 78

75 Zhang L, Peng C T, Shi J *et al. Journal of Alloys and Compounds*[J], 2020, 828: 154460

76 Gao X L, Liu H, Liu J *et al. Journal of Materials Processing Technology*[J], 2019, 270: 293

77 Ning J, Hong K M, Inamke G V *et al. Journal of Manufacturing Processes*[J], 2019, 39: 146

78 Zhang L L, Zhang L J, Long J *et al. Materials & Design*[J], 2019, 169: 107681

79 Luo M Z, Liang L, Lang L *et al. Computational Materials Science*[J], 2018, 141: 293

80 Yu X J, Kumar K S. *Materials Science and Engineering A*[J], 2016, 676: 312
81 Zhang Liang, Long Weimin, Zhong Sujuan *et al. Rare Metal Materials and Engineering*[J], 2022, 51(10): 3905 (in Chinese)
82 Li J F, Cheng J G, Wei B Z *et al. International Journal of Refractory Metals and Hard Materials*[J], 2017, 66: 226
83 Yao G, Liu X, Zhao Z *et al. Materials & Design*[J], 2021, 212: 110249
84 Sun H H, Wang M, Xi X L *et al. Materials Science and Engineering A*[J], 2021, 824: 141806
85 Wang Y, Gao J C, Chen G M *et al. International Journal of Refractory Metals and Hard Materials*[J], 2008, 26(1): 9
86 Sıralı H, Şimşek D, Özyürek D. *Metals and Materials International*[J], 2021, 27: 4110
87 Browning P N, Fignar J, Kulkarni A *et al. International Journal of Refractory Metals and Hard Materials*[J], 2017, 62: 78
88 Cui C P, Gao Y M, Wei S Z *et al. High Temperature Materials and Processes*[J], 2017, 36(2): 167
89 Hu P, Zuo Y G, Li S L *et al. Journal of Alloys and Compounds*[J], 2021, 870: 159429
90 Sun T L, Xu L J, Wei S Z *et al. International Journal of Refractory Metals and Hard Materials*[J], 2020, 86: 105085
91 Wang C, Wang P, Hou Q Y *et al. Fusion Engineering and Design*[J], 2023, 188: 113420
92 Min G, Oh Y, Kim H *et al. Journal of Alloys and Compounds*[J], 2023, 953: 169961
93 Lan X, Li Z B, Zhang H *et al. International Journal of Refractory Metals and Hard Materials*[J], 2023, 110: 106014
94 Li W H, Zhang G J, Wang S X *et al. Journal of Alloys and Compounds*[J], 2015, 642: 34
95 Zhao Y, Long W M, Huang S *et al. Rare Metal Materials and Engineering*[J], 2023, 51(12): 4502
96 Zhou W, Sun X, Kikuchi K *et al. Materials & Design*[J], 2018, 146: 116
97 Yang L L, Zhang Q F, He Z Y *et al. International Journal of Refractory Metals and Hard Materials*[J], 2017, 67: 56
98 Zhang T Q, Wang Y J, Zhou Y *et al. Materials Science and Engineering A*[J], 2010, 527(16-17): 4021
99 Hu W, Kong X, Du Z *et al. Journal of Alloys and Compounds*[J], 2021, 859: 157774
100 Zhang Liang, Long Weimin, Zhong Sujuan *et al. Rare Metal Materials and Engineering*[J], 2022, 51(9): 3492 (in Chinese)
101 Hu W Q, Du Z F, Dong Z Z *et al. Scripta Materialia*[J], 2021, 198: 113831
102 Zhao J, Liu L C, Gong H R *et al. Surface and Coatings Technology*[J], 2020, 382: 125158
103 Cui D T, Zhong S J, Song K X *et al. Rare Metal Materials and Engineering*[J], 2021, 50(6): 1935
104 Zhang L L, Zhang L J, Ning J *et al. Journal of Manufacturing Processes*[J], 2021, 68: 1637
105 Zhang L J, Yu H, Zeng X L *et al. Optics & Laser Technology*[J], 2024, 175: 110749

钨/钼合金先进焊接技术研究现状

王星星[1]，楚浩强[1]，谢　旭[1]，潘昆明[2]，杜全斌[3]，李　昂[3]，张黎燕[3]
(1. 华北水利水电大学 河南高效特种绿色焊接国际联合实验室，河南 郑州 450045)
(2. 龙门实验室，河南 洛阳 471003)
(3. 河南机电职业学院 河南省超硬材料智能制造装备集成重点实验室，河南 郑州 451191)

摘　要：钨/钼合金因其高熔点、高强度等特性，在核工业、航空航天等领域中广泛应用。然而，其烧结性、加工性较差，在制造大尺寸或复杂形状零件时极为困难，因此开展钨/钼合金先进焊接技术研究非常必要。从钨/钼合金焊接缺陷和焊接工艺出发，介绍近年钎焊、放电等离子烧结扩散焊、电子束焊、激光焊等特种连接技术及合金掺杂处理应用于钨/钼合金异质连接的最新进展，同时指出钨/钼合金焊接存在的问题。最后对钨/钼合金各种焊接技术的未来发展进行总结和展望，为钨/钼合金焊接技术进一步发展提供理论支撑和工程依据。

关键词：钨合金；钼合金；焊接技术；微观组织；力学性能

作者简介：王星星，男，1984年生，博士，教授，华北水利水电大学河南省高效特种绿色焊接国际联合实验室，河南 郑州 450045，E-mail：wangxingxing@ncwu.edu.cn